

Ensuring Safety in Target Pursuit Control: A CBF-Safe Reinforcement Learning Approach

Yaosheng Deng, Junjie Gao, Jiaping Xiao and Mir Feroskhan.

Abstract—This paper addresses the target-pursuit problem, aiming to ensure each pursuer’s safety regarding collision avoidance, sensing range, and input saturation. An input-constrained Control Barrier Function (CBF) is proposed to dynamically regulate the pursuer’s control, ensuring effective target pursuit even when the target performs evasive maneuvers. To further ensure safety, two sets of CBF constraints are designed to regulate the pursuer’s position, enabling it to keep the target within the sensing range while avoiding collision in complex environments with external disturbances. These three CBFs collectively form our safety filter, which filters unsafe outputs from RL by solving a Quadratic Program (QP). Finally, the safety filter, combined with a switch strategy that enhances the feasibility of solving its QP, constitutes the CBF-Safe Reinforcement Learning (CSRL) algorithm, whose solutions are proven to satisfy the Karush-Kuhn-Tucker (KKT) conditions for all safety constraints. Simulation results validate the effectiveness of the CSRL algorithm, demonstrating its ability to handle complex pursuit scenarios while maintaining safety and improving control performance.

Index Terms—Multi-agent System, CBF, safety filter.

I. INTRODUCTION

Target pursuit problems are fundamental in robotics and control theory, with potential applications such as wireless charging of electric vehicles [1], [2], wildlife monitoring [3], [4], and defense against malicious UAVs [5]. A critical challenge in target pursuit lies in simultaneously addressing three safety factors: sensing safety, collision avoidance, and input constraints. Specifically, the pursuit agent must maintain uninterrupted sensing of the target to ensure accurate real-time tracking, even in the presence of external disturbances. Furthermore, the pursuit agent often operates in complex environments, where it is crucial to achieve collision avoidance without compromising continuous sensing of the target. Lastly, the agent’s input and velocity constraints must allow it to pursue a non-cooperative target effectively, particularly when the target accelerates to evade capture. These considerations highlight the need for a systematic framework that guarantees multiple safety factors in pursuing target scenarios.

Several traditional methodologies have been extensively explored in target pursuit problems. In [6], a Lyapunov-based approach is proposed to ensure asymptotic convergence of the UAV to the target’s neighborhood, demonstrating its effectiveness in achieving stable tracking. However, it does not account for additional challenges that arise during pursuit, such as collision avoidance and input safety constraints, limiting its applicability in more complex environments. In [7], a model predictive control (MPC)-based algorithm dynamically adjusts UAVs along the target’s trajectory, demonstrating its

effectiveness in collision avoidance. However, a significant limitation of MPC in pursuit control lies in its computational complexity, which can result in delays and, consequently, the loss of target tracking [8]. In [9], a rapidly exploring random tree-based approach was employed for pursuing the target in a static environment. However, this method lacks the ability to update paths in real-time, resulting in potential tracking failures in complex environments [10]. In summary, these traditional methods may struggle to balance safety constraints and performance in target pursuit problems due to limitations in computational efficiency.

To address the computational inefficiencies in the target pursuit problem, end-to-end approaches, such as reinforcement learning (RL), offer the advantage of faster computation [5]. However, external disturbances and unseen scenarios beyond the training data pose significant challenges to system safety in RL pursuit control. To address these issues, safety filter methods, which transform RL outputs into safe control signals [11], have gained significant attention for ensuring system safety. For example, in [12], a predictive-based filter achieved safe UAV pursuit control. However, the feasible path required a long predictive horizon, leading to high computational costs, with limited improvement over traditional prediction control methods [13]. In [14], a CBF-based filter is applied to any potentially unsafe signal, ensuring forward invariance of the safe set without incurring additional computational costs. However, a single-form CBF may struggle to simultaneously address multiple objectives such as obstacle avoidance, target tracking, and input constraints [15]. In [16], an MPC-CBF-based safety filter was proposed to target pursuit tasks with input constraints, exploring the input space over multiple time steps. However, this approach transforms the originally convex QP problem into a nonlinear programming problem due to CBF discretization, significantly increasing computational complexity. These limitations highlight the importance of verifying the feasibility of CBF-based terminal safety filters, particularly in target pursuit tasks that involve multiple safety factors and external disturbances.

In this paper, we propose a CSRL algorithm to ensure safe and efficient target pursuit by addressing collision avoidance, sensing range, and input saturation constraints in a complex environment with external disturbance. The CSRL algorithm framework includes a trained RL model for target pursuit, a safety filter constructed from three adaptive CBF constraints, and a switch strategy that selects between the RL output and the safety filter’s control signals. To design our algorithm, we first augment the system by introducing virtual control inputs, which transform the input-constrained problem into an output-constrained problem, enhancing the feasibility of the associated QP. Based on the pursuer’s position and velocity, we then construct the safety filter using three adaptive CBFs, ensuring that unsafe RL outputs are converted into safe

Mir Feroskhan is the corresponding authors.

Yaosheng Deng, Junjie Gao, Jiaping Xiao, and Mir Feroskhan are with the School of Mechanical and Aerospace Engineering, Nanyang Technological University, Singapore, Singapore 639798 (e-mail: yaosheng001@e.ntu.edu.sg; junjie008@e.ntu.edu.sg; jiaping001@e.ntu.edu.sg; mir.feroskhan@ntu.edu.sg).

control inputs even under external disturbances. Finally, we incorporate a switch strategy to alternate between RL actions and the safety filter, and we prove that the proposed switch strategy ensures the safety filter satisfies the KKT conditions for each safety constraint, guaranteeing the overall feasibility of the CSRL algorithm. The main contributions of this paper are summarized as follows:

- We address input constraints by augmenting the system with virtual control inputs and designing an input-constrained CBF based on this framework. This approach, unlike conventional constant constraints [17], [18], enforces general input bounds while adaptively relaxing the upper limits in special scenarios, such as when the target accelerates evasively, thereby providing the pursuer with sufficient maneuverability.
- We design two position-based CBFs to ensure collision avoidance and sensing range safety. Together with the input-constrained CBF, these CBFs form a safety filter, which is solved as a QP problem. We incorporate an adaptive-based technique into the safety filter, enabling each pursuer to maintain safety in complex environments, even under external unknown disturbances.
- We propose the CSRL algorithm, centered on a switch strategy that determines the safety of RL outputs and switches between the RL output and the safety filter accordingly. Unsafe RL outputs are converted into safe control inputs by solving a QP problem. Finally, we prove that the CSRL algorithm satisfies the KKT conditions for all safety constraints of each pursuer.

The rest of the paper is organized as follows. Section II presents some preliminaries. Section III formulates the pursuit control problem, including the system dynamics, safety constraints, and problem objectives. Section IV presents the proposed CSRL algorithm, detailing the input-constrained CBF, the safety filter, and the switch strategy. The theoretical guarantees of the algorithm are also provided in this section. Section V validates the proposed method through simulations, demonstrating its effectiveness in ensuring safety and performance under various scenarios. Finally, Section VI concludes the paper and discusses potential directions for future work.

II. PRELIMINARY

Let \mathbb{R} , \mathbb{R}^+ denote the field of real numbers and the set of non-negative reals. For a vector $x \in \mathbb{R}^n$, x_i denotes the i -th element of x , $\|x\| = \sqrt{x_1^2 + \dots + x_n^2}$ denotes the two-norm of x . Let M be a matrix, define $\lambda_{\min} M$ as the minimum eigenvalue of a matrix M . A continuous function $\alpha : [0, a) \rightarrow [0, \infty)$ is class- \mathcal{K} for some $a > 0$ if it is strictly increasing on the domain, and $\alpha(0) = 0$. It is class- \mathcal{K}_∞ if $\lim_{r \rightarrow \infty} \alpha(r) \rightarrow \infty$.

A. CBF

Consider the following control affine system

$$\dot{x}(t) = f(x) + g(x)u(t), \quad (1)$$

where, $x \in \mathbb{R}^n$ is the state variable, $u \in \mathbb{R}^m$ denotes the control input of (1). f and g are locally Lipschitz continuous.

Definition 1. [19] Let

$$\mathcal{C} = \{x \in \mathbb{R}^n : h(x) \geq 0\}, \quad (2)$$

where $h : \mathbb{R}^n \rightarrow \mathbb{R}$ is a continuously differentiable function. Set $\mathcal{C} \subset \mathbb{R}^n$ is forward invariant for system (1) if its solutions starting at all $x(t_0) \in \mathcal{C}$ satisfy $x(t) \in \mathcal{C}$ for all $t \geq t_0$.

Definition 2. [20] Given a set \mathcal{C} as in (2), $h(x)$ is a CBF for system (1) if there exists a class \mathcal{K} function γ such that

$$L_f h(x) + L_g h(x)u + \gamma(h(x)) \geq 0 \quad (3)$$

for all $x \in \mathcal{C}$.

B. High-order CBF (HOCBF)

In the context of high-order control barrier functions, first, we introduce relative degree:

Definition 3. A continuously differentiable function h is said to have relative degree r on a given domain of x with respect to system (1) if $L_g L_f^k h(x) = 0$ for all $k < r-1$ and $L_g L_f^r h(x) \neq 0$ hold for all $x \in \mathbb{R}^n$.

While Definition 2 is only applicable to CBFs with a relative degree of one, many applications often involve CBFs with higher relative degrees. To accommodate such scenarios, an extended definition known as HOCBFs has been developed in [21]. In this approach, we define a series of continuously differentiable functions $\tilde{h} : \mathbb{R}^n \rightarrow \mathbb{R}$ as

$$\begin{aligned} \tilde{h}_1(x) &= h(x), \\ \tilde{h}_i(x) &= \dot{\tilde{h}}_{i-1}(x) + \alpha(\zeta_{i-1}(x)), i \in \{1, \dots, r\}, \end{aligned} \quad (4)$$

We also define their zero-superlevel sets \mathcal{C}_i and their interior sets for $i \in \{1, \dots, r\}$ as

$$\mathcal{C}_i = \{x \in \mathbb{R}^n \mid \tilde{h}_{i-1}(x) \geq 0\}. \quad (5)$$

Definition 4. Let the functions $\zeta_i(x)$ and sets \mathcal{C}_i be defined by (4) and (5), respectively. The r -th order continuously differentiable function $h(x)$ with relative degree $r > 1$ is called a HOCBF if h and its derivatives up to order r , are locally Lipschitz continuous such that

$$\begin{aligned} \sup_{u \in \mathbb{R}^m} \left[L_f^r h + L_g L_f^{r-1} h u + \sum_{i=1}^{r-1} L_f^i (\alpha \circ \tilde{h}_{r-i-1}) \right. \\ \left. + \alpha(\tilde{h}_{r-1}) \right] \geq 0, \end{aligned} \quad (6)$$

for all $x \in \bigcap_{i=1}^r (\mathcal{C}_i)$.

III. PROBLEM STATEMENT

This paper aims to design a safe algorithm for the target pursuing problem with collision avoidance, sensing limitation, and input constraint. The algorithm design is based on the following safe strategy.

A. Safe Strategy for Pursuers

Consider a group of n pursuit agents and n target agents. Let $x_i \in \mathbb{R}^n$ where $i \in \mathcal{I}_x = \{1, \dots, N\}$ be the position of the i -th pursuit agent and $\mathcal{X} = \{x_i\}$ denotes a collection of functions of x_i . Let $q_i \in \mathbb{R}^n$, $i \in \mathcal{I}_q = \{1, \dots, N\}$, be the position of the i -th target agent and $\mathcal{Q} = \{q_i\}$ denotes a collection of functions of q_i . Note that the i -th pursuer's primary task is tracking the corresponding target position q_i . Suppose the sensing range of each pursuit agent is $R_i \in \mathbb{R}^+$, then the sensing safe for i -th pursuer should satisfy

$$\|p_i(t) - q_i(t)\| \leq R_i, \quad (7)$$

for all $i \in \mathcal{I}_x$ and $t \geq 0$.

Similar to the agents, the environment obstacles $j \in \mathcal{I}_o = \{1, \dots, M\}$ are also modeled as a rigid sphere at $o_j \in \mathcal{O} \subset \mathbb{R}^{n,M}$. Let $\mathcal{P} = \mathcal{X} \cup \mathcal{Q} \cup \mathcal{O}$ denote the set of all agents and obstacles. To describe the i -th pursuit agent's collision avoidance requirements, define $\mathcal{P}_{-i} = \mathcal{P} \setminus \{x_i\}$ as the set of all agents excluding x_i . The safe distance between the position of i -th pursuer x_i and the position $p_k \in \mathcal{P}_{-i}$ should satisfy

$$\|x_i(t) - p_k(t)\| \geq r_i, \quad (8)$$

for all $k \in \mathcal{I}_k = \{1, \dots, 2N + M - 1\}$ and all $t \geq 0$. Next, we made the following assumption for the observation of p_k .

Assumption 1. *The velocity and acceleration of the k -th agent, \dot{p}_k and \ddot{p}_k , are bounded by two positive constraint $\rho_v \in \mathbb{R}^+$ and $\rho_a \in \mathbb{R}^+$, such that $\|\dot{p}_k(t)\| \leq \rho_v$, and $\|\ddot{p}_k(t)\| \leq \rho_a$ for all $k \in \mathcal{I}_k$ and $t \geq 0$.*

B. Statement of Problem

The following control affine system governs the position vector x_i of the i -th pursuit agent:

$$\dot{x}_i(t) = f(x_i) + g(x_i)u_i(t) + Y(x_i)\theta, \quad (9)$$

where $x_i \in \mathbb{R}^n$ is the state of i -th pursuer, $u_i \in \mathbb{R}^m$ is its control input. $f(x_i)$ is the drift term, and $g(x_i)$ is the control matrix, both of which are locally Lipschitz continuous functions of x_i . $Y : \mathbb{R}^n \rightarrow \mathbb{R}^{n \times p}$ represents known locally Lipschitz lumped uncertainties, and $\theta \in \mathbb{R}^p$ is a constant vector of uncertain parameters.

Let $u_{\text{nom},i}$ denote the nominal control input of system (9), which is designed to achieve the primary objective of system (9), such as target tracking or stabilization. It represents the control input in the absence of safety constraints and governs the behavior of the i -th pursuer as

$$\dot{x}_i(t) = f(x_i) + g(x_i)u_{\text{nom},i}(t) + Y(x_i)\theta, \quad (10)$$

One specific form of $u_{\text{nom},i}$ can be:

$$u_{\text{nom},i}(t) = \int_0^t \pi_i(x_i(\tau))d\tau, \quad (11)$$

where $\pi_i(x_i)$ is a continuous control law derived, for example, from model-free RL [22] or optimization-based methods [23]. However, directly applying $u_{\text{nom},i}$ in system (10) can lead to unsafe behaviors, such as violating input limits, collision constraints, or sensing requirements. To mitigate these risks, we first introduce a time-varying input constraint $\kappa = \kappa(x_i(t))$ for the i -th pursuer to regulate its control input u_i

$$\|u_i(t)\| \leq \kappa(x_i(t)), \quad (12)$$

for all $t \geq 0$. To enforce this input constraint, we define an input constraint safe set for system (9) using the CBF technique. Specifically, a Lipschitz continuous function $h_{u,i}$ is defined as an input constraint CBF.

$$h_{u,i}(x_i, u_i, t) = \kappa(x_i(t))^2 - \|u_i(t)\|^2, \quad (13)$$

and the input constraint safe set for the i -th pursuer is defined as:

$$\mathcal{C}_{u,i} = \{u_i \in \mathbb{R}^m \mid h_{u,i}(x_i, u_i, t) \geq 0\}. \quad (14)$$

Unlike conventional single-target pursuit problems, this paper considers N target-pursuer pairs in an environment with M obstacles. In such a complex scenario, each pursuer must

ensure sensing range safety as in (7) while simultaneously maintaining collision avoidance by satisfying the safe radius condition in (8). These dual safety requirements necessitate the formulation of appropriate safety constraints. Therefore, we introduce the collision avoidance safety set $\mathcal{C}_{c,i}$ and sensing range safety set $\mathcal{C}_{s,i}$ for each pursuer i as follows:

$$\mathcal{C}_{c,i} = \bigcap_{k \in \mathcal{I}_k} \{x_i \in \mathbb{R}^n \mid h_{c,i,k}(x_i(t)) \geq 0\}, \quad (15)$$

$$\mathcal{C}_{s,i} = \{x_i \in \mathbb{R}^m \mid h_{s,i}(x_i(t)) \geq 0\}, \quad (16)$$

where $h_{c,i,k}$ and $h_{s,i}$ are two Lipschitz continuous function with a relative degree 2 defined as

$$h_{c,i,k}(t) = \|x_i(t) - p_k(t)\|^2 - r_i^2, \quad (17)$$

$$h_{s,i}(t) = R_i^2 - \|x_i(t) - q_i(t)\|^2. \quad (18)$$

Together with the input constraint set $\mathcal{C}_{u,i}$ in (14), the collision avoidance set $\mathcal{C}_{c,i}$ in (15) and sensing range set $\mathcal{C}_{s,i}$ in (16) collectively describe the safety requirements for each pursuer.

Now we can state the problem studied in this paper.

Problem 1. *Given the target-pursuit system governed by (9), where each pursuer follows its dynamics. Design the safe control law u_i for all $i \in \mathcal{I}_x$ such that safety sets $\mathcal{C}_{u,i}$ in (14), $\mathcal{C}_{c,i}$ in (15), and $\mathcal{C}_{s,i}$ in (16) forward invariant for all $t \geq 0$.*

IV. METHODOLOGY

In this section, we present the design of the CSRL algorithm to solve Problem 1. The proposed approach begins by transforming the original system into an augmented system, reformulating the input-constrained problem into an output-constrained problem. To ensure forward invariance of the safety sets \mathcal{C}_u , \mathcal{C}_c , and \mathcal{C}_s for the pursuers, an adaptive CBF-based safety filter is developed, providing robustness against external disturbances. Finally, the CBF-based safety filter is integrated with a model-free RL policy into the CSRL algorithm. We demonstrate that the CSRL algorithm guarantees feasibility and ensures sensing safety, collision avoidance, and compliance with input constraints for all pursuit agents.

A. System transform

To provide time-varying bounds on the actual control variable u , it is natural to place an integrator in the feedback path to augment the system's output as the input of an auxiliary system. Specifically, by introducing an integrator for the control input u , the original first-order system in (9) is transformed into a second-order system, where the time derivative of u is treated as a new auxiliary input v . As a result, the system can now be described as:

$$\begin{aligned} \dot{x}_i(t) &= f(x_i(t)) + g(x_i(t))u_i(t) + Y(x_i(t))\theta \\ \dot{u}_i(t) &= v_i(t) + Z(x_i(t))\xi, \end{aligned} \quad (19)$$

where $v_i \in \mathbb{R}^n$ is an auxiliary input vector. $\xi \in \mathbb{R}$ is the unknown uncertainty, and $Z \in \mathbb{R}^m$ is a local Lipschitz functions.

Remark 1. *The uncertainty in the system (19) will always be regarded as sensor faults polluting all the states [24], [25], which addresses that all the states including u_i are polluted due to sensor faults coinciding in each system state, which is of theoretical and practical significance.*

To facilitate our approach, we make the following assumption on the structure of the uncertainty in (19)

Assumption 2. *The uncertain parameters θ and ξ belong to the known convex polytope $\theta \in \Theta \subset \mathbb{R}^p$ and $\xi \in \Xi \subset \mathbb{R}^p$, so that there exists the maximum possible estimation error $\varepsilon_\theta, \varepsilon_\xi \in \mathbb{R}^+$ such that $\|\theta - \hat{\theta}\| \leq \varepsilon_\theta$ and $\|\xi - \hat{\xi}\| \leq \varepsilon_\xi$.*

Then, to deal with the uncertainty in the augmented system (19), the following Lemma, adapted from [26], provides a verifiable bound on the estimations $\hat{\theta}$ and $\hat{\xi}$, based on the following adaptive law.

Lemma 1. *Let $t_j \in [t - \Delta T, t] \subset \mathbb{R}$, $j \in \{1, \dots, M\}$ be the j -th sampling time. M represents the total sampling times. Given the adaptive law for system (19) as follows*

$$\dot{\hat{\theta}}(t) = \gamma_\theta \sum_{j=1}^M \mathcal{Y}_i(t_j)^\top \left(\Delta x_{i,j}(t_j) - \mathcal{Y}_i(t_j) \hat{\theta}(t_j) - \mathcal{F}_i(t_j) - \mathcal{G}_i(t_j) \right), \quad (20)$$

$$\dot{\hat{\xi}}(t) = \gamma_\xi \sum_{j=1}^M \mathcal{Z}_i(t_j)^\top \left(\Delta x_{i,j}(t_j) - \mathcal{Z}_i(t_j) \hat{\xi} - \mathcal{V}_i(t_j) \right), \quad (21)$$

where, $\Delta x_{i,j}(t) = x_i(t_j) - x_i(t_j - \Delta T)$, $\mathcal{F}_i(t_j) = \int_{t_j - \Delta T}^{t_j} f(x_i(\tau)) d\tau$, $\mathcal{Y}_i(t_j) = \int_{t_j - \Delta T}^{t_j} Y(x_i(\tau)) d\tau$, $\mathcal{G}_i(t_j) = \int_{t_j - \Delta T}^{t_j} g(x_i(\tau)) u_i(\tau) d\tau$, $\mathcal{Z}_i(t_j) = \int_{t_j - \Delta T}^{t_j} Z(x_i(\tau)) d\tau$ and $\mathcal{V}_i(t_j) = \int_{t_j - \Delta T}^{t_j} v_i(\tau) d\tau$. $\gamma_\theta \in \mathbb{R}^+$ and $\gamma_\xi \in \mathbb{R}^+$ are adaptation gains. Provided Assumption 2 holds and $\hat{\theta}(0) \in \Theta$, $\hat{\xi}(0) \in \Xi$, then the parameter estimation error $\tilde{\theta}$ and $\tilde{\xi}$ are bounded by two positive constant $\bar{\nu} \in \mathbb{R}^+$ and $\bar{\eta} \in \mathbb{R}^+$

$$\begin{aligned} \|\tilde{\theta}(t)\| &\leq \bar{\nu} \\ \|\tilde{\xi}(t)\| &\leq \bar{\eta}, \end{aligned} \quad (22)$$

for all $t \geq 0$.

Remark 2. *Using Assumption 2 and Theorem 2 in [27] to (22), the positive constants $\bar{\nu}$ and $\bar{\eta}$ in Lemma 1 satisfy*

$$\begin{aligned} \bar{\nu} &\geq \|\varepsilon_\theta\| e^{-\gamma_\theta \int_0^t \lambda_\theta(\tau) d\tau} \\ \bar{\eta} &\geq \|\varepsilon_\xi\| e^{-\gamma_\xi \int_0^t \lambda_\xi(\tau) d\tau}, \end{aligned} \quad (23)$$

for all $t \geq 0$, where

$$\lambda_\theta(t) = E_{\min} \sum_{j=1}^M \mathcal{Y}_i(t_j)^\top \mathcal{Y}_i(t_j), \quad (24)$$

$$\lambda_\xi(t) = E_{\min} \sum_{j=1}^M \mathcal{Z}_i(t_j)^\top \mathcal{Z}_i(t_j), \quad (25)$$

The above lemma implies that, under the updated law in (20) and (21), the parameter estimation error is always bounded by a known value provided the initial parameter estimates are selected such that $\hat{\theta}(0) \in \Theta$ and $\hat{\xi}(0) \in \Xi$. These bounded errors enable the development of a robust safety filter to ensure the forward invariance of safety sets $\mathcal{C}_{u,i}$ in (14), $\mathcal{C}_{c,i}$ in (15), and $\mathcal{C}_{s,i}$ in (16), even in the presence of system uncertainties.

B. Safety Filter Design

In this subsection, we design auxiliary input v_i to regulate the system in (19), ensuring that $\mathcal{C}_{u,i}$ in (14), $\mathcal{C}_{c,i}$ in (15), and $\mathcal{C}_{s,i}$ in (16) remain forward invariant even in the presence of system uncertainties. To achieve this, we construct three adaptive CBFs for each safety requirement, leveraging the parameter estimation error derived in Lemma 1. Then, we formulate three CBF conditions as a QP problem, whose solution yields the safety filter's output.

Building on this framework, the input constraint for the pursuer is designed to address two key aspects. The first component is a static constraint, which serves as a baseline to filter extreme RL actions, ensuring smooth and safe control inputs. The second component is a dynamic, time-varying constraint that activates during critical scenarios (e.g. $\|x_i - q_i\| - R_i \rightarrow 0$). Thus we define the following input-constrained CBF based on the relative positions between the pursuer and the target, denoted by $\zeta_i = x_i - q_i$, as follows

$$h_{u,i}(t) = \kappa(\zeta_i(t))^2 - u_i(t)^2, \quad (26)$$

where,

$$\kappa(\zeta_i(t)) = c + \frac{1}{(\zeta_i^\top \zeta_i - \ell^2)^2 + \epsilon}, \quad (27)$$

with positive constants $c > 0$, $\epsilon > 0$, and $\ell > 0$.

Remark 3. *The formulation (27) represents a time-varying input constraint that dynamically adapts based on the relative position of the i -th pursuer x_i to its target q_i , ensuring that the input signal remains appropriately regulated, thereby guaranteeing safety even under critical scenarios such as target evasive maneuvers or simultaneous obstacle avoidance and tracking.*

Building on the augmented system in Section IV-A, we now proceed to ensure the safety sets $\mathcal{C}_{c,i}$, $\mathcal{C}_{s,i}$ and $\mathcal{C}_{u,i}$ forward invariant for all $x_i \in \mathcal{X}$, $i \in \mathcal{I}_x$. Specifically, we design the auxiliary controller v_i for system (19), such that CBFs defined by (26), (17) and (18) satisfy $h_{c,i}(t) \geq 0$, $h_{s,i}(t) \geq 0$, and $h_{u,i}(t) \geq 0$ for all $i \in \mathcal{I}_x$ and $t \geq 0$. For simplicity of notations, we denote $f_i = f(x_i)$, $g_i = g(x_i)$, $Y_i = Y(x_i)$, $Z_i = Z(x_i)$, and omit the time variable t in the rest of the paper.

The following lemma provides conditions under which the input constraint safety set $\mathcal{C}_{u,i}$ forward invariant.

Lemma 2. *Suppose Assumption 1 and Assumption 2 holds for all $i \in \mathcal{I}_x$ and $t \geq 0$. Let the parameter estimation error be bounded as in Lemma 1, and define the set of admissible control inputs for the i -th pursuer as:*

$$K_{u,i}(x_i, u_i, \hat{\theta}, \hat{\xi}) = \sup_{v_i \in \mathbb{R}^m} \left\{ L_{u,i} - u_i^\top v_i + \alpha(h_{u,i}) \geq 0 \right\}, \quad (28)$$

where

$$\begin{aligned} L_{u,i}(x_i, u_i, \hat{\theta}, \hat{\xi}) &= \frac{-2\kappa(\zeta_i^\top \zeta_i - \ell^2)}{(\zeta_i^\top \zeta_i - \ell^2)^2 + \epsilon} \zeta_i^\top (f_i + g_i u_i + Y_i \hat{\theta}) - u_i^\top Z_i \hat{\xi} \\ &\quad - \left\| \frac{2\kappa(\zeta_i^\top \zeta_i - \ell^2)}{(\zeta_i^\top \zeta_i - \ell^2)^2 + \epsilon} \zeta_i \right\| (\|Y_i\| \nu + \rho_v) \\ &\quad - \|u_i^\top Z_i\| \eta. \end{aligned} \quad (29)$$

Then, any Lipschitz continuous controller $v_i \in K_{u,i}(x_i, \hat{\theta}, \hat{\xi})$ guarantees the forward invariance of set $\mathcal{C}_{u,i}$ in (14) regarding to system (19) for all $x_i \in \mathbb{R}^n$, $\theta \in \Theta$, $\xi \in \Xi$ and $t \geq 0$.

The proof of this lemma 2 is provided in the Appendix.

With the safety of the control input ensured by Lemma 2, we now extend our analysis to derive safe conditions for collision avoidance. Given a position of i -th pursuer x_i , the objective is to ensure

$$\varkappa_k(t) = \|x_i(t) - p_k(t)\| \geq r_i, \quad (30)$$

for all $k \in \mathcal{I}_k$ and all $t \geq 0$. The following lemma provides sufficient conditions of forward invariant of the safety set $\mathcal{C}_{c,i}$, which indicates the i -th pursuer is collision-free.

Lemma 3. Let $\iota_k \in \mathbb{R}^+$ be a positive constant for all $k \in \mathcal{I}_k$. Suppose Assumption 1 and Assumption 2 holds. Let the parameter estimation error be bounded as in Lemma 1, and define the set of admissible control inputs for the i -th pursuer as:

$$\begin{aligned} & K_{c,i,k}(x_i, \hat{\theta}, \hat{\xi}) \\ &= \sup_{v_i \in \mathbb{R}^m} 2 \left\{ L_{c,i,k} - \varkappa_k^\top g_i v_i + \alpha_k(h_{i,k}(x_i)) \geq 0 \right\}, \end{aligned} \quad (31)$$

where

$$\begin{aligned} & L_{c,i,k}(x_i, \hat{\theta}, \hat{\xi}) \\ &= \varkappa_k^\top (\dot{f}_i + \dot{g}_i u_i) + \varkappa_k^\top \dot{Y}_i \hat{\theta} - \left\| \varkappa_k^\top \dot{Y}_i \right\| \nu - \|\varkappa_k\| \rho_a \\ & \quad + \varkappa_k^\top g_i Z_i \hat{\xi} - \left\| \varkappa_k^\top g_i Z_i \right\| \eta \\ & \quad + \iota_k \left(\varkappa_k^\top (f_i + g_i u_i) + \varkappa_k^\top Y_i \hat{\theta} \right. \\ & \quad \left. - \left\| \varkappa_k^\top Y_i \right\| \nu \right). \end{aligned} \quad (32)$$

Then any Lipschitz continuous controller $v_i \in K_{c,i} = \bigcap_{k \in \mathcal{I}_k} K_{c,i,k}$ renders the safety of $\mathcal{C}_{c,i}$ forward invariant for all $k \in \mathcal{I}_k$, $\theta \in \Theta$, $\xi \in \Xi$ and all $t \geq 0$.

The proof of this lemma 3 is provided in the Appendix.

Subsequently, the conditions to ensure the safety of the sensing range $\mathcal{C}_{s,i}$ in (16) are derived based on the relative position $\zeta_i = x_i - q_i$ between the pursuer and the target, as stated in Lemma 4.

Lemma 4. Let $\iota_t \in \mathbb{R}^+$ be a positive constant. Suppose Assumption 1 and Assumption 2 holds for all $t \geq 0$. Let the parameter estimation error be bounded as in Lemma 1, and define the set of admissible control inputs for the i -th pursuer as:

$$\begin{aligned} & K_{s,i}(x_i, \hat{\theta}, \hat{\xi}) \\ &= \sup_{v_i \in \mathbb{R}^m} 2 \left\{ L_{s,i} + \zeta_i^\top g_i v_i - \alpha_t(h_{s,i}(x_i)) \geq 0 \right\}. \end{aligned} \quad (33)$$

where

$$\begin{aligned} & L_{s,i}(\zeta_i, \hat{\theta}, \hat{\xi}) \\ &= -\iota_t \zeta_i^\top (f_i + g_i u_i) - \zeta_i^\top (\iota_t Y_i + \dot{Y}_i) \hat{\theta} + \|\zeta_i\| \rho_a \\ & \quad - \zeta_i^\top (\dot{f}_i + \dot{g}_i u_i) - \zeta_i^\top g_i Z_i \hat{\xi} + \left\| \zeta_i^\top g_i Z_i \right\| \eta \\ & \quad + \left(\left\| \iota_t \zeta_i^\top Y_i \right\| + \left\| \zeta_i^\top \dot{Y}_i \right\| \right) \nu. \end{aligned} \quad (34)$$

Then any Lipschitz continuous controller $v_i \in K_{s,i}$ renders the safety of $\mathcal{C}_{s,i}$ forward invariant for all $x_i \in \mathbb{R}^n$, $\theta \in \Theta$, $\xi \in \Xi$ and all $t \geq 0$.

Since the proof of Lemma 4 is analogous to that of Lemma 3, it is omitted here. The above Lemmas 2, 3, and 4 collectively establish that the proposed safety constraints—collision avoidance, sensing range, and input constraint—are forward invariant under appropriate control input designs for each pursuer in the target-pursuit system (19). Building on these results, we construct a CBF-QP formulation that integrates the trained RL action $\pi_i(t)$ as the nominal control input for pursuer i at time t . This formulation ensures compliance with the safety constraints established in Lemmas 2, 3, and 4, yielding the safety adaptive controller v_i^* , as follows:

CBF-QP Problem for Pursuer i

$$\begin{aligned} & v_i^*(t) = \arg \min_{v_i \in \mathbb{R}^m} \frac{1}{2} \|v_i(t) - \pi_i(t)\|^2 \\ & \text{s.t.} \end{aligned} \quad (35)$$

$$v_i \in K_{u,i}(x_i, u_i, \hat{\theta}, \hat{\xi}) \cap K_{c,i}(x_i, \hat{\theta}, \hat{\xi}) \cap K_{s,i}(x_i, \hat{\theta}, \hat{\xi}).$$

Given the above CBF-QP problem, it is essential to investigate the feasibility of the proposed safety filter. Specifically, we aim to integrate the RL control input π_i with the safety filter into a unified algorithm, ensuring that when the RL input violates safety conditions, the safety filter is activated and remains feasible for each safety requirement.

C. CSRL Algorithm

In this part, we propose the overall framework of our CSRL algorithm for the pursuer control problem, which integrates model-free RL with a safety filter to ensure the satisfaction of the safety constraints $\mathcal{C}_{u,i}$ in (14), $\mathcal{C}_{c,i}$ in (15) and $\mathcal{C}_{s,i}$ in (16). Specifically, there is a switch strategy in our CSRL algorithm that switches between the RL action π_i and the safety filter in (35), depending on whether the safety filter is activated. To formalize the feasibility of this framework, we present the main theorem of this paper, which proves the switch strategy ensures the CBF-QP problem satisfies the safety conditions in Lemmas 2, 3, and 4, whenever the safety filter is activated. Consequently, the proposed CSRL algorithm guarantees that the pursuer control problem stated in Problem 1 is fully satisfied.

Given the above CBF-QP problem in (35), it is necessary to develop a feasible continuous control law to satisfy each safety condition. To achieve this, we introduce a switch strategy π_i that activates the safety filter in (35) by switching from the nominal RL action π_i whenever a CBF constraint is violated. For this purpose, we define the following regions:

$$\begin{aligned} & \Pi_{u,i} = \left\{ u_i \in \mathcal{C}_{u,i} \mid L_{u,i} + \alpha h_{u,i} - u_i^\top \pi_i \geq 0 \right\}, \\ & \Pi_{s,i} = \left\{ x_i \in \mathcal{C}_{s,i} \mid L_{s,i} + \alpha h_{s,i} - \zeta_i^\top g_i \pi_i \geq 0 \right\}, \\ & \Pi_{c,i} = \left\{ x_i \in \mathcal{C}_{c,i} \mid \bigcap_{k \in \mathcal{I}_k} \left(L_{c,i,k} + \alpha h_{c,i,k} \right. \right. \\ & \quad \left. \left. - \varkappa_k^\top g_i \pi_i \geq 0 \right) \right\}, \end{aligned} \quad (36)$$

which represents the case when nominal RL action π_i is safe for rendering the safety sets forward invariant. Then we define

$$\mathcal{R}_1 = \left\{ (x_i, u_i) \mid (u_i \in \Pi_{u,i}) \cap (x_i \in (\Pi_{c,i} \cap \Pi_{s,i})) \right\}, \quad (37)$$

and

$$\mathcal{R}_2 = -\mathcal{R}_1. \quad (38)$$

Obviously, when $(x_i, u_i) \in \mathcal{R}_1$, the safety filter is inactive since $v_i = \pi_i$, and when $(x_i, u_i) \in \mathcal{R}_2$, we solved the safe control v_i^* by QP problem in (35). Therefore, we proposed the following hybrid control law:

$$\phi_i(x_i, u_i) = \begin{cases} \pi_i(x_i, u_i) & \text{if } (x_i, u_i) \in \mathcal{R}_1 \\ v_i^*(x_i, u_i) & \text{if } (x_i, u_i) \in \mathcal{R}_2 \end{cases}. \quad (39)$$

Now we can show the main Theorem for the feasibility of (35).

Theorem 1. *If the initial conditions of (17), (18) and (26) hold for*

$$\bar{h}_{c,i,k}(0) > 0, \quad \bar{h}_{s,i}(0) > 0, \quad \bar{h}_{u,i}(0) > 0, \quad (40)$$

and given the hybrid control law $\phi_i(x_i, u_i)$ in (39). Then the QP problem in (35) is feasible for each CBF conditions and has a unique solution of $x_i \in (\bigcap_{k \in \mathcal{I}_k} \mathcal{C}_{c,i,k}) \cap \mathcal{C}_{s,i}$ and $u_i \in \mathcal{C}_{u,i}$ for all $i \in \mathcal{I}_x$ and $t \geq 0$.

Proof. To determine the feasibility of maintaining these constraints simultaneously, we construct the Lagrangian function:

$$\begin{aligned} L_i(v_i, \lambda_i, \lambda_{s,i}, \lambda_{u,i}) \\ = \frac{1}{2} \|v_i - \pi_i\|^2 - \sum_{k \in \mathcal{I}_k} \lambda_{i,k} \bar{h}_{c,i,k} - \lambda_{s,i} \bar{h}_{s,i} - \lambda_{u,i} \bar{h}_{u,i}, \end{aligned} \quad (41)$$

where $\lambda_{i,k}$, $\lambda_{s,i}$, and $\lambda_{u,i}$ should always satisfy dual feasibility s.t. $\lambda_{i,k}, \lambda_{s,i}, \lambda_{u,i} \geq 0$, $i \in \mathcal{I}$, are the Lagrange multipliers associated with each constraint. According to the KKT conditions, the solutions of the QP program are optimal and unique if the following stationary condition

$$\begin{aligned} \frac{\partial L_i}{\partial v_i} \\ = (v_i - \pi_i) - \sum_{k \in \mathcal{I}_k} \lambda_{c,i,k} \frac{\partial \bar{h}_{c,i,k}}{\partial v_i} - \lambda_{s,i} \frac{\partial \bar{h}_{s,i}}{\partial v_i} - \lambda_{u,i} \frac{\partial \bar{h}_{u,i}}{\partial v_i} \end{aligned} \quad (42)$$

$$= 0,$$

and complementary slackness

$$\begin{aligned} \lambda_{s,i}(L_{s,i} + \alpha h_{s,i} + \zeta_i^\top g_i v_i) &= 0, \\ \lambda_{u,i}(L_{u,i} + \alpha h_{u,i} + u_i^\top v_i) &= 0 \\ \sum_{k \in \mathcal{I}_k} \lambda_{c,i,k}(L_{c,i,k} + \alpha h_{c,i,k} + \varkappa_k^\top g_i v_i) &= 0, \end{aligned} \quad (43)$$

hold with respect to v_i . Additionally, we define the active set \mathcal{A}_j , $j = \{1, 2, 3\}$ for the QP problem in (35) as the set of constraints that are active at a given solution v_i^* , i.e., the constraints for which the equality $\bar{h}_{c,i,k} = 0$, $\bar{h}_{s,i} = 0$, or $\bar{h}_{u,i} = 0$ holds. For all inactive constraints, the corresponding inequality holds $\bar{h}_{c,i,k} > 0$, $\bar{h}_{s,i} > 0$, and $\bar{h}_{u,i} > 0$.

To analyze the feasibility of the QP problem, we individually consider each constraint being active while others are inactive. Specifically, there are three cases to be considered:

Case 1: $\mathcal{A}_1 = \{k \in \mathcal{I}_k \mid \bar{h}_{c,i,k}(v_i) = 0\}$.

For $\varkappa_k \in \mathcal{R}_2$ the KKT conditions result in

$$v_i - \pi_i - \sum_{k \in \mathcal{I}_k} \lambda_{i,k} \varkappa_k^\top g_i = 0 \quad (44a)$$

$$\sum_{k \in \mathcal{I}_k} \lambda_{c,i,k}(L_{c,i,k} + \alpha h_{c,i,k} + \varkappa_k^\top g_i v_i) = 0 \quad (44b)$$

$$\lambda_{c,i,k} \geq 0 \quad (44c)$$

for all $k \in \mathcal{I}_k$. Using hybrid control law in (39), we have

$$L_{c,i,k} + \alpha h_{c,i,k}(x_i) - \varkappa_k^\top g_i \pi_i \leq 0 \quad (45)$$

Apply (44b) to (44a), we obtains

$$v_i = -\frac{L_{c,i,k} + \alpha h_{c,i,k}(x_i)}{\|\varkappa_k^\top g_i\|^2} g_i^\top \varkappa_k, \quad (46)$$

and the stationarity conditions of (44a)

$$-\frac{L_{c,i,k} + \alpha h_{c,i,k}(x_i)}{\|\varkappa_k^\top g_i\|^2} g_i^\top \varkappa_k - \pi_i - \sum_{k \in \mathcal{I}_k} \lambda_{i,k} \varkappa_k^\top g_i = 0. \quad (47)$$

Using (45) to (47), the following inequality is obtained

$$\sum_{k \in \mathcal{I}_k} \lambda_{i,k} = -\left(\frac{L_{c,i,k} + \alpha h_{c,i,k}(x_i)}{\|\varkappa_k^\top g_i\|^2} g_i^\top \varkappa_k + \pi_i \right) \frac{g_i^\top \varkappa_k}{\|\varkappa_k^\top g_i\|^2} \quad (48)$$

$$\begin{aligned} \sum_{k \in \mathcal{I}_k} \lambda_{i,k} \\ = -\left(\frac{L_{c,i,k} + \alpha h_{c,i,k}(x_i)}{\|\varkappa_k^\top g_i\|^2} g_i^\top \varkappa_k + \pi_i \right) \frac{g_i^\top \varkappa_k}{\|\varkappa_k^\top g_i\|^2} \\ = -\frac{L_{c,i,k} + \alpha h_{c,i,k}(x_i)}{\|\varkappa_k^\top g_i\|^2} + \pi_i \frac{g_i^\top \varkappa_k}{\|\varkappa_k^\top g_i\|^2} \\ \geq -\frac{L_{c,i,k} + \alpha h_{c,i,k}(x_i)}{\|\varkappa_k^\top g_i\|^2} + \frac{L_{c,i,k} + \alpha h_{c,i,k}(x_i)}{\|\varkappa_k^\top g_i\|^2} \\ \geq 0, \end{aligned} \quad (49)$$

which implies the active set $\mathcal{A}_1 = \{k \in \mathcal{I}_k \mid \bar{h}_{c,i,k}(v_i) = 0\}$ is valid for all $k \in \mathcal{I}_k$. Since the KKT conditions are met and the unique solution for the QP problem in (35) is given by (46), the QP problem is feasible for all $x_i \in \mathcal{R}_2$ under the validated active set \mathcal{A}_1 .

Case 2: $\mathcal{A}_2 = \{\bar{h}_{s,i}(v_i) = 0\}$.

For $\zeta_i \in \mathcal{R}_2$ the KKT conditions result in

$$v_i - \pi_i - \lambda_{s,i} \zeta_i^\top g_i = 0, \quad (50a)$$

$$\lambda_{s,i}(L_{s,i} + \alpha h_{s,i} + \zeta_i^\top g_i v_i) = 0, \quad (50b)$$

$$\lambda_{s,i} \geq 0. \quad (50c)$$

Using hybrid control law in (39), we have

$$L_{s,i} + \alpha h_{s,i}(x_i) - \zeta_i^\top g_i \pi_i \leq 0 \quad (51)$$

Apply (50b) to (50a), we obtains

$$v_i = -\frac{L_{s,i} + \alpha h_{s,i}(x_i)}{\|\zeta_i^\top g_i\|^2} g_i^\top \zeta_i, \quad (52)$$

Using (51) to (50a), the following inequality is obtained

$$\begin{aligned} \lambda_{s,i} = -\left(\frac{L_{s,i} + \alpha h_{s,i}(x_i)}{\|\zeta_i^\top g_i\|^2} g_i^\top \zeta_i + \pi_i \right) \frac{g_i^\top \zeta_i}{\|\zeta_i^\top g_i\|^2} \\ \geq 0, \end{aligned} \quad (53)$$

which implies the active set $\mathcal{A}_2 = \{\bar{h}_{s,i}(v_i) = 0\}$ is valid for all $\zeta_i \in \mathcal{R}_2$. Since the KKT conditions are met and the unique solution for the QP problem in (35) is given by (52), the QP problem is feasible for all $x_i \in \mathcal{R}_2$ under the validated active set \mathcal{A}_2 .

Case 3: $\mathcal{A}_3 = \{\bar{h}_{u,i}(v_i) = 0\}$.

For $u_i \in \mathcal{R}_2$ the KKT conditions result in

$$v_i - \pi_i - \lambda_{u,i} u_i = 0, \quad (54a)$$

$$\lambda_{u,i} (L_{u,i} + \alpha h_{u,i} + u_i^\top v_i) = 0, \quad (54b)$$

$$\lambda_{u,i} \geq 0. \quad (54c)$$

Using hybrid control law in (39), we have

$$L_{u,i} + \alpha h_{u,i}(x_i) - u_i^\top \pi_i \leq 0 \quad (55)$$

Apply (54b) to (54a), we obtains

$$v_i = -\frac{L_{u,i} + \alpha h_{u,i}(x_i)}{\|u_i\|^2} u_i^\top, \quad (56)$$

Using (55) to (54a), the following inequality is obtained

$$\lambda_{u,i} = -\left(\frac{L_{u,i} + \alpha h_{u,i}(x_i)}{\|u_i\|^2} u_i^\top + \pi_i\right) \frac{u_i^\top}{\|u_i\|^2} \geq 0, \quad (57)$$

which implies the active set $\mathcal{A}_i = \{\tilde{h}_{u,i}(v_i) = 0\}$ is valid for all $u_i \in \mathcal{R}_2$. Since the KKT conditions are met and the unique solution for the QP problem in (35) is given by (52), the QP problem is feasible for all $u_i \in \mathcal{R}_2$ under the validated active set \mathcal{A}_3 .

Lastly, we prove the Lipschitz continuity of v_i^* for all $(x_i, u_i) \in \mathcal{R}_2$. The coefficient matrix of the CBF-QP problem in (35) is given by

$$V(x_i, u_i) = \begin{bmatrix} u_i^\top \\ -\zeta_i^\top g_i \\ -\sum_{k \in \mathcal{I}_k} \varkappa_k^\top g_i \end{bmatrix}. \quad (58)$$

Following Theorem 3.1 of [28] and given that the solution in (46), (52) and (56) are well defined as $\varkappa_k^\top g_i$, $\zeta_i^\top g_i$ and u_i is bounded away from 0 in any bounded subset of \mathcal{R}_2 as $h_{c,i,k}$, $h_{s,i}$ (relative degree 2), and $h_{u,i}$ are CBFs for system (19). Therefore, the matrix $V(x_i, u_i)$ is full rank, ensuring v_i^* is Lipschitz continuous for all $(x_i, u_i) \in \mathcal{R}_2$. Since the CBF-QP problem in (35) is utilized as part of the hybrid control law in (39), and thus it is only employed for $(x_i, u_i) \in \mathcal{R}_2$ to compute a control input. For $(x_i, u_i) \in \mathcal{R}_1$, the nominal RL action is safe and the CBF constraints are inactive. Therefore, using Corollary 3.3 of [29], the hybrid control law $\phi(x_i, u_i)$ in (39) is continuous for all $x_i \in (\bigcap_{k \in \mathcal{I}_k} \mathcal{C}_{c,i,k}) \cap \mathcal{C}_{s,i}$ and $u_i \in \mathcal{C}_{u,i}$ for any $i \in \mathcal{I}_x$ and $t \geq 0$ thus completing the proof. \square

Building on Theorem 1, which establishes the feasibility of the hybrid control law in satisfying the safety constraints (15), (16) and (14), we now present the framework of our CSRL algorithm for our pursuit control problem. The CSRL algorithm integrates the safety filter with model-free RL, ensuring that each pursuer can safely pursue its target with the sensing limitations and input constraints while avoiding collisions with obstacles and other agents. The complete framework is outlined in Algorithm 1.

V. EXPERIMENTS

In this section, we design a set of numerical simulations involving two target-pursuit multicopter experiments to verify the effectiveness and safety of the proposed method. Specifically, two follower UAVs operate in the same environment, each tasked with tracking a corresponding target UAV,

Algorithm 1: CSRL Algorithm for Target Pursuit Control

- Input:** Environment dynamics f, g ;
 Safety constraints $\mathcal{C}_u, \mathcal{C}_t, \mathcal{C}_c$;
 m Static obstacles $\mathcal{O} = \{o_1, \dots, o_m\}$;
 n Pursuer $\mathcal{X} = \{x_1, \dots, x_n\}$;
 n Target $\mathcal{Q} = \{q_1, \dots, q_n\}$;
 n Trained RL policy $\pi_i, i = \{1, \dots, n\}$;
 Environment disturbances θ, ξ .
Output: $x_i \in (\bigcap_{k \in \mathcal{I}_k} \mathcal{C}_{c,i,k}) \cap \mathcal{C}_{s,i}$ and $u_i \in \mathcal{C}_{u,i}$.
- 1) Initialize n pursuers $\mathcal{X}(0) = \{x_1(0), \dots, x_n(0)\}$, n targets $\mathcal{Q}(0) = \{q_1(0), \dots, q_n(0)\}$, and m static obstacles $\mathcal{O} = \{o_1(0), \dots, o_m(0)\}$.
 - 2) Set initial parameters for each pursuer $x_i(0), u_i(0), f_i(0), g_i(0), Y_i(0), Z_i(0), \hat{\theta}(0), \hat{\xi}(0), i \in \mathcal{I}_x$.
 - 3) For each time step t :
 - a) Get $\mathcal{P}_{-i} = \{p_1 \dots p_{2n+m-1}\} = (\mathcal{X} \setminus x_i) \cup \mathcal{Q} \cup \mathcal{O}$,
 - b) Compute relative positions:
 - Target distance $\zeta_i = x_i - q_i$,
 - Relative positions to other targets, pursuers, and obstacles $\varkappa_k = x_i - p_k$.
 - c) Evaluate hybrid control law $\phi(x_i, u_i)$ using (39).
 - d) **If** safety filter is activated:
 - Compute auxiliary control input v_i^* by solving the CBF-QP problem in (35).
 - Auxiliary control input $v_i = v_i^*$.
 - e) **Else:** Auxiliary control input $v_i = \pi_i(x_i)$.
 - f) Compute x_i and u_i from v_i by dynamics (19).
-

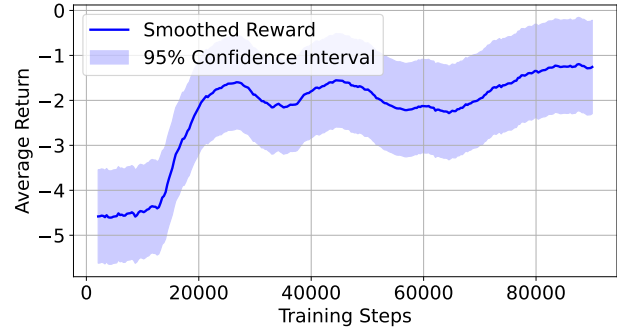


Figure 1: The average return training curves of SAC by running 3 times with different seeds. The lines and shaded areas represent the average return and the 95% confidence interval, respectively.

while navigating around obstacles and subject to unknown disturbances. To achieve this, we adopt the Soft Actor-Critic (SAC) [30], an off-policy, model-free reinforcement learning algorithm, as the nominal control input for the followers.

In the model-free RL framework, the control action π_i is generated by the SAC policy for the i -th pursuer, which is trained to enable a follower agent to maintain a specified tracking range from its target in an obstacle-free environment without disturbances. The objective is to develop an RL control strategy for tracking that can later be integrated with safety constraints. To train the SAC policy for the pursuer's control actions, the reward function $r(x_i, \pi_i)$ is designed to encourage the i -th pursuer's position x_i remaining within a desired distance range $[r_1, R_1]$ to the target position p_0 . The reward

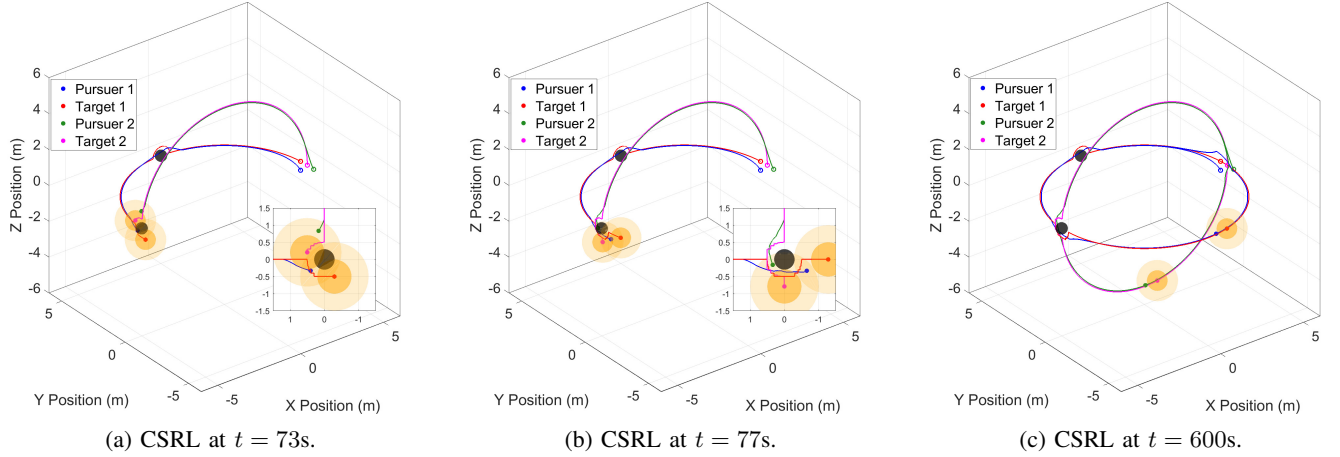


Figure 2: Snapshots of the CSRL algorithm at $t = 73s$, $77s$, and $600s$ during the first experiment where the targets perform circular maneuvers. The red and magenta trajectories represent two pursuer agents, while the blue and green trajectories represent two target agents. The dark yellow spheres indicate the target safety radius $r_i = 0.5$, and the light yellow spheres denote the sensing range between the pursuer and its target $R_i = 1.0$. Black spheres represent static obstacles with a radius of 0.3 . Hollow circles in corresponding colors represent the initial positions of each agent.

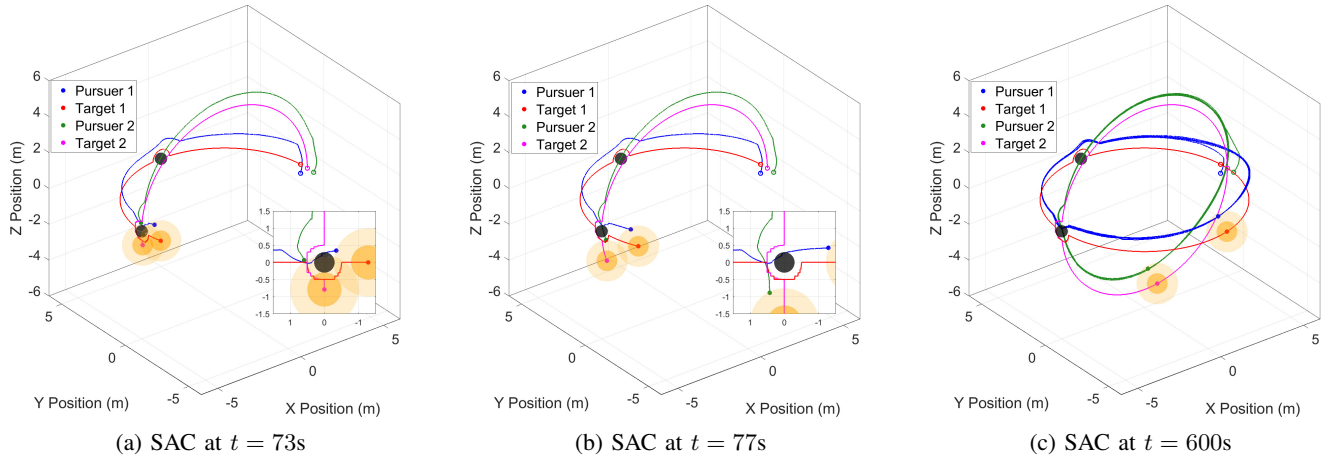


Figure 3: Snapshots of the only use SAC for pursuit agents at $t = 73s$, $77s$, and $600s$ where the targets perform circular maneuvers.

function is formulated as:

$$r(x_i, \pi_i) = \begin{cases} 0.1 & \text{if } r_i \leq \|\zeta_i\| \leq R_i, \\ -0.1\|\zeta_i\| - r_i & \text{if } \|\zeta_i\| < r_i, \\ -0.1\|\zeta_i\| - R_i & \text{if } \|\zeta_i\| > R_i. \end{cases} \quad (59)$$

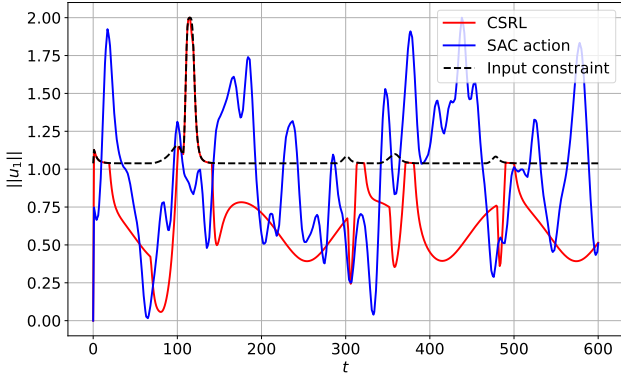
The reward function (59) is designed to capture the relationship between tracking error and reward, assigning larger rewards for small errors and diminishing rewards as the error increases. This structure prevents the reward from approaching zero for large errors, aiding numerical stability and discouraging significant deviations from the target. The SAC policy is trained over 1500 episodes and the time interval between each step is $0.1s$ for each dimension of pursuer's acceleration. Figure 1 illustrates the average return training curves for the SAC algorithms. The results indicate that training a SAC-based target pursuit controller fails due to the challenges of balancing multiple safety constraints during target maneuvers, which significantly increases the training complexity and can lead to failure. To ensure safety, the CBF-QP-based algorithm (35), as outlined in Algorithm 1, is employed for two pursuit agents

after training, enabling safe tracking of their respective targets while accounting for disturbances, obstacles, sensing range and input saturation.

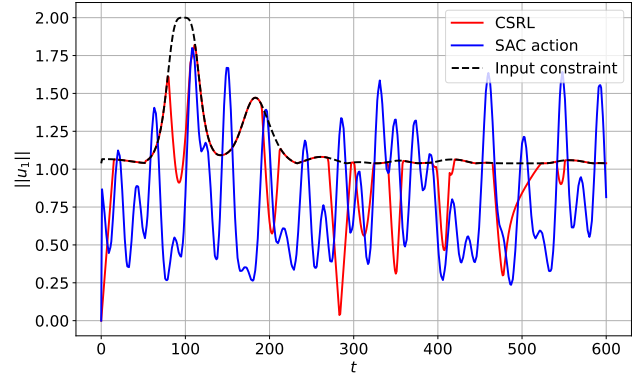
For simplicity, we set the uncertain viscous friction functions $Y_i\theta = \sin(x_i)$, $Z_i\xi = \cos(x_i)$, with uncertain coefficients $\theta = \xi = 1$ for all pursuit agents. Two sphere obstacles are placed and their specific positions of center $p_1 = [4.70, 3.25, 3.00]$; $p_2 = [-4.20, 3.00, 4.75]$. The safe radius is set as $r_i = 0.5$ and $R_i = 1$ for all $i \in \mathcal{I}_x$. The total time of this simulation is 600 steps and the time step is set as 0.1 . The movement law of the first target $p_{0,1}$, and second target $p_{0,2}$ is defined as

$$\begin{aligned} \dot{p}_{0,1} &= \ddot{p}_{r1} + (p_{r1} - p_{0,1}) + (p_{r1} - \dot{p}_{0,1}) + U_1(x), \\ \dot{p}_{0,2} &= \ddot{p}_{r2} + (p_{r2} - p_{0,2}) + (p_{r2} - \dot{p}_{0,2}) + U_2(x), \end{aligned} \quad (60)$$

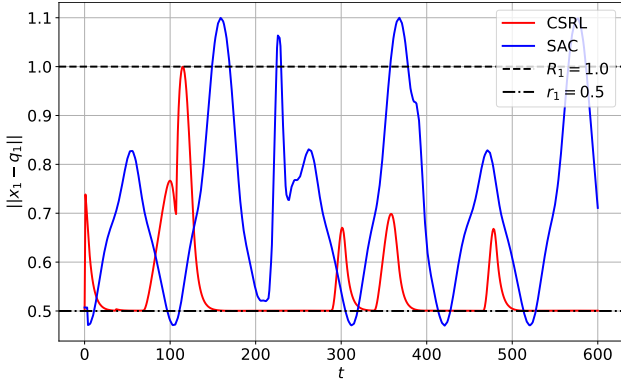
where $U_j(x) = \sum_{i=1}^2 \left(\frac{1}{\|p_0 - p_i\|} - 0.1 \right) \frac{p_{0,j} - p_i}{\|p_0 - p_i\|^3}$, $j \in \{1, 2\}$, is a potential field term for target agent collision-avoidance to obstacle p_1 and p_2 , and p_{r1} , p_{r2} in (60) are the reference signal for target agents. In our first experiment, the



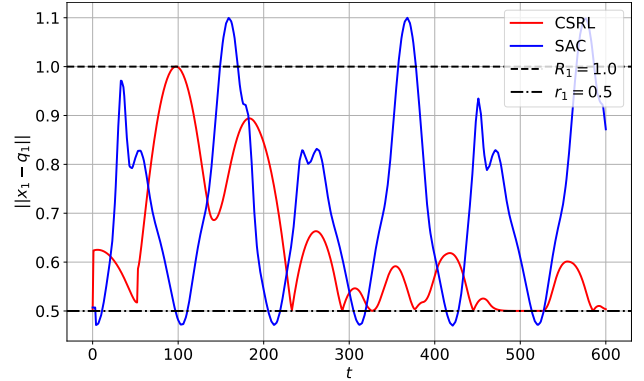
(a) The control input u_1 of CSRL and RL only with time-varying input constraint κ .



(b) The control input u_2 of CSRL and SAC only with time-varying input constraint κ .

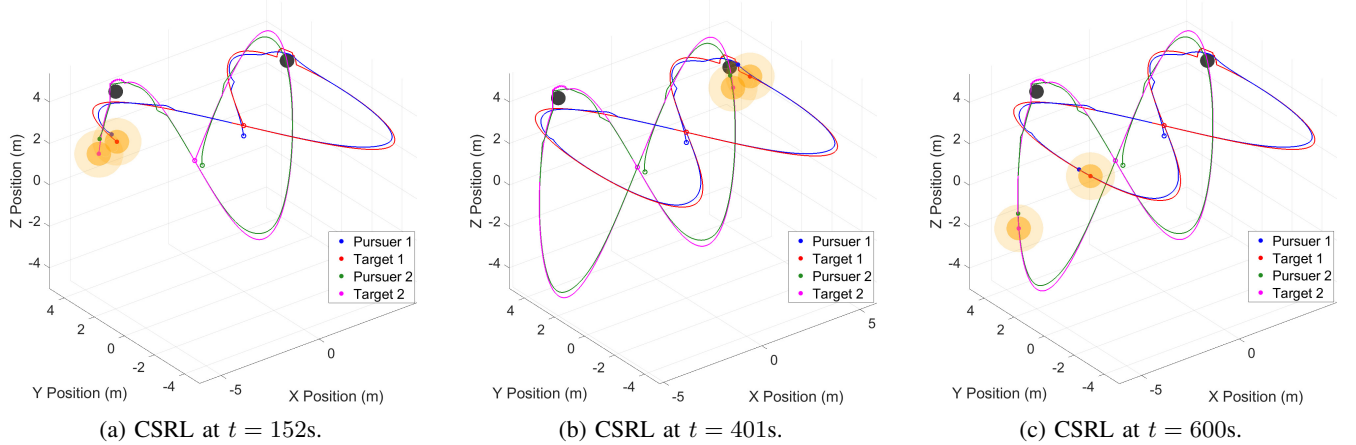


(c) The distance $\|x_1 - q_1\|$ of CSRL and SAC only with safe collision radius $r_1 = 0.5$ and safe sensing radius $R_1 = 1.0$.



(d) The distance $\|x_2 - q_2\|$ of CSRL and SAC only with safe collision radius $r_2 = 0.5$ and safe sensing radius $R_2 = 1.0$.

Figure 4: Comparison of the CSRL algorithm and SAC-only control in terms of control input u_i and relative distance $\|\zeta_i\| = \|x_i - q_i\|$ for pursuer agents 1 and 2.



(a) CSRL at $t = 152s$.

(b) CSRL at $t = 401s$.

(c) CSRL at $t = 600s$.

Figure 5: Snapshots of the CSRL algorithm at $t = 152s$, $401s$, and $600s$ where the targets perform “figure-8” maneuvers.

targets follow a large circular maneuver, with their positions updated as: $p_{r1} = [5 \sin(0.1t), 5 \cos(0.1t), 0]$ and $p_{r2} = [5 \sin(0.1t), 0, 5 \cos(0.1t)]$. In our second experiment, the targets follow a “figure-8” reference signal [31], given by: given by $p_{r1} = [5 \sin(0.1t), 5 \sin(0.2t), 3]$ and $p_{r2} = [5 \sin(0.1t), 3, 5 \sin(0.2t)]$.

In the first experiment, we evaluated the proposed CSRL algorithm 1 with two targets following large circular maneuvers as shown in Figure 2. The targets incorporated a potential

field term in (60) for collision avoidance with obstacles. From Figure 5(a), both target-pursuer pairs converge near $[-5; 0; 0]$, where a radius 0.3 obstacle is present. The targets perform large-angle maneuvers guided by the potential field term in (60). Close-up views indicate that all pursuers maintain safe distances from obstacles and other agents, while retaining sensing of their corresponding targets at $t = 73s$. Then from Figure 2(b), the pursuers successfully navigate around the obstacle while maintaining sensing safety with their respective

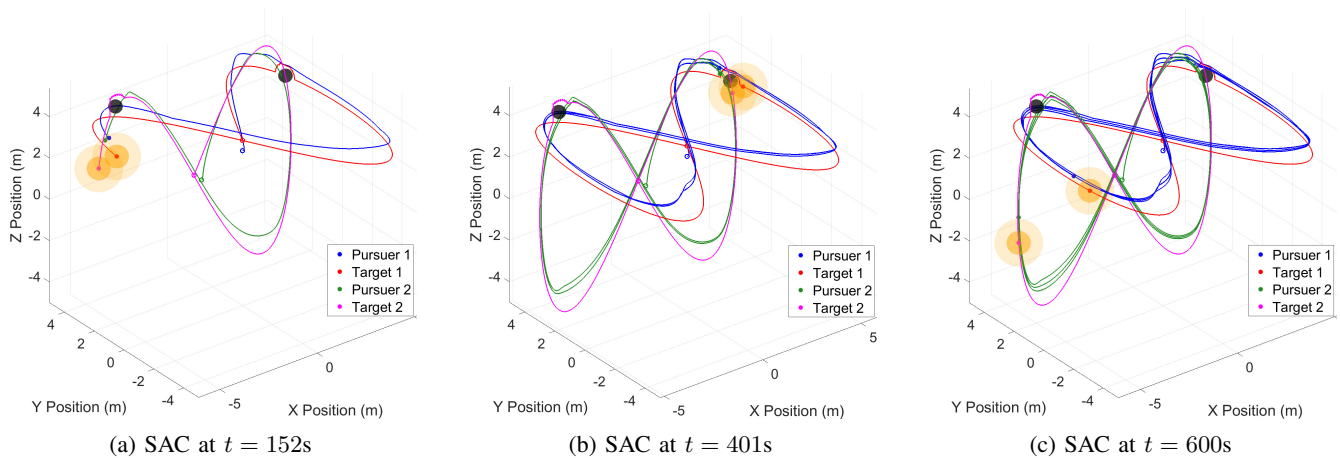
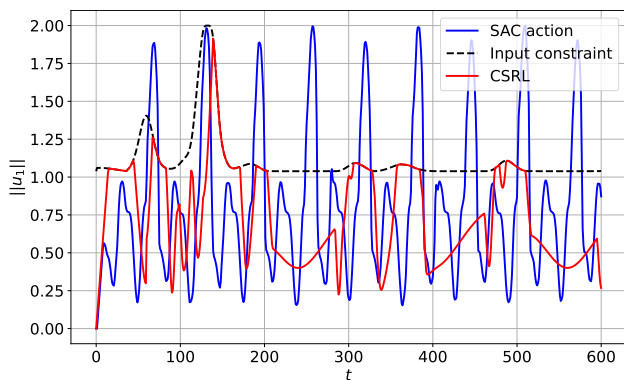
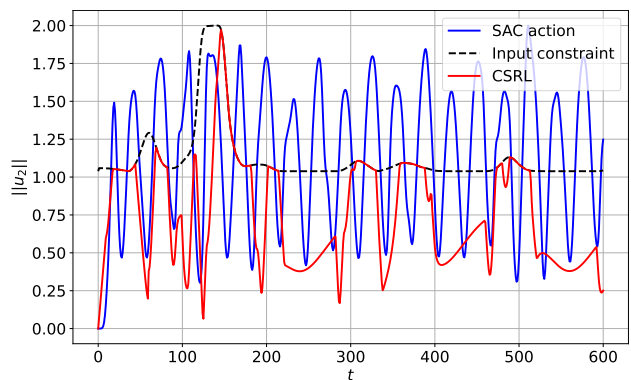


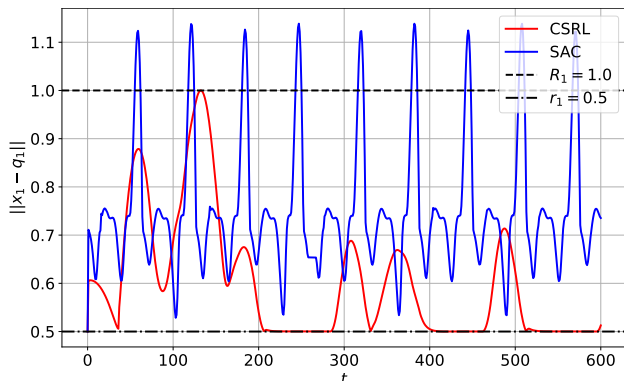
Figure 6: Snapshots of the only use SAC as the RL controller for pursuit agents at $t = 152s$, $401s$, and $600s$ where the targets perform “figure-8” maneuvers.



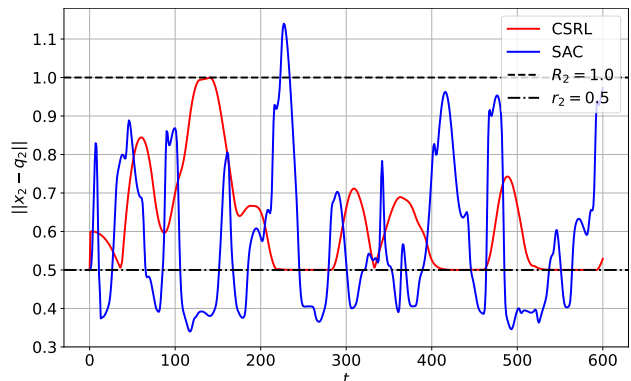
(a) The control input u_1 of CSRL and SAC only with time-varying input constraint κ .



(b) The control input u_2 of CSRL and SAC only with time-varying input constraint κ .



(c) The distance $\|x_1 - q_1\|$ of CSRL and SAC only with safe collision radius $r_1 = 0.5$ and safe sensing radius $R_1 = 1.0$.



(d) The distance $\|x_2 - q_2\|$ of CSRL and SAC only with safe collision radius $r_2 = 0.5$ and safe sensing radius $R_2 = 1.0$.

Figure 7: Comparison of the CSRL algorithm and SAC-only control in terms of control input u_i and relative distance $\|\zeta_i\| = \|x_i - q_i\|$ for pursuer agents 1 and 2.

targets. In Figure 2(c) the trajectories of both pursuers remain relatively stable under external disturbances, ensuring reliable tracking of their targets. Figure 3 presents a comparison with the SAC-only method. In Figure 3(a), the blue pursuer collides with the obstacle, highlighting the inability of SAC to guarantee collision safety. In Figure 3(b), both pursuers fail to maintain sensing safety, as the distances between pursuers and their respective targets exceed the sensing range $R_i = 1$

(indicated by the light yellow region). From Figure 3(c) we observe that under external disturbances, the SAC algorithm demonstrates unstable tracking behavior, failing to reliably pursue the targets. These results demonstrate the superior performance of the CSRL algorithm in ensuring collision safety, sensing safety, and tracking stability, even in challenging scenarios with obstacles and disturbances, compared to the SAC-only method. Figure 4 is the data plot corresponding to

the scenario in Figure 2 and Figure 3, where Figure 4(a) and Figure 4(b) demonstrates that, compared to the SAC algorithm, the proposed CSRL algorithm ensures that the control inputs of both pursuers consistently satisfy the input constraints in (14) throughout the target pursuit process. Figure 4(c) and Figure 4(d) illustrate that, under the CSRL algorithm, both pursuers maintain sensing safety (16) and collision safety (15) with their respective targets, which are not guaranteed under the SAC algorithm.

To evaluate the algorithm's performance in more dynamic environments, we conducted a second set of experiments where the target agents followed "figure-8" trajectory. These trajectories introduce varying curvature and dynamic changes, providing a more challenging test for the CSRL algorithm. Figure 5 shows our proposed algorithm 1 by two groups of pursuit agents tracking the corresponding target agents with "figure-8-shape" reference signal. It can be obtained that our algorithm ensures the safe sensing range $[r_i, R_i]$ and collision-avoidance of both follower 1 to target 1 and follower 2 to target 2. From Figure 5(a), at $t = 152s$, the two pursuer agents maintain a safe distance from each other while tracking their respective targets $\|x_1 - x_2\| = 0.5162 > 0.5$. In contrast, Figure 6(a) shows that the SAC-only method fails to maintain the safe collision radius between the pursuers ($0.2822 < 0.5$). In Figure 5(b), at $t = 401s$, the two pursuer agents not only avoid obstacles but also maintain sensing of their respective targets. However, in Figure 6(b), it is evident that both pursuer 1 and pursuer 2 lose sensing of their targets, highlighting the limitation of the RL-only method. Finally, comparing Figure 5(c) and Figure 6(c), it is clear that under external disturbances θ and ξ , the proposed CSRL algorithm demonstrates superior tracking stability compared to the SAC-only method, ensuring reliable pursuit control even in challenging scenarios.

Figures 7(a) and 7(b) demonstrate that under the CSRL algorithm, both pursuer 1 and pursuer 2 maintain their control inputs within the input constraint κ in the second experiment. Around $t = 125s$, when the targets exhibit evasive maneuvers, the input constraint temporarily increases to accommodate the stronger control effort required to ensure sensing safety. During normal tracking phases, the input constraint effectively regulates the control input, preventing unstable nominal control signals and ensuring smooth operation. Figures 7(c) and 7(d) show that the CSRL algorithm enables both pursuer 1 and pursuer 2 to maintain the required safe collision radius and sensing range with their respective target agents. This ensures that the pursuers achieve safe and effective target tracking, even under challenging conditions. The results validate that the CSRL algorithm not only satisfies input constraints and safety requirements $\mathcal{C}_{u,i}$ in (14), $\mathcal{C}_{c,i}$ in (15) and $\mathcal{C}_{s,i}$ in (16) for all pursuit agents, but also improves the stability and robustness of target pursuit, making it suitable for scenarios with external disturbances and dynamic targets.

VI. CONCLUSION

In this paper, we proposed a CSRL algorithm to address the target-pursuit problem, ensuring safety regarding collision avoidance, sensing range, and input saturation in complex environments with external disturbances. The algorithm integrates three CBF constraints—input-constrained, collision-avoidance, and sensing-range constraints—into a safety filter that transforms unsafe RL outputs into safe control signals via a QP. A switched strategy further enhances the feasibility of

solving the safety filter's QP, ensuring solutions satisfy the KKT conditions for all safety constraints. This work provides a framework for safe and reliable target-pursuit operations in complex and dynamic environments, with potential applications in UAV surveillance and wireless charging of electric vehicles.

ACKNOWLEDGMENT

The authors would like to express their sincere gratitude to the honorable Prof. Yang Bai, from the Graduate School of Advanced Science and Engineering, Hiroshima University, for his constructive feedback and insightful discussions, which greatly contributed to the improvement of this work.

APPENDIX

The proof of Lemma 2 is provided as follows.

Proof. Let $\zeta_i = x_i - q_i$. The derivative of $h_{u,i}$ is given by

$$\begin{aligned} \dot{h}_{u,i} &= \frac{1}{2}(\kappa\dot{\kappa} - u_i^\top \dot{u}_i) \\ &= -\frac{2\kappa(\zeta_i^\top \zeta_i - \ell^2)}{(\zeta_i^\top \zeta_i - \ell^2)^2 + \epsilon^2} \zeta_i^\top (f_i + g_i u_i - \dot{q}_i) \\ &\quad - \frac{2\kappa(\zeta_i^\top \zeta_i - \ell^2)}{(\zeta_i^\top \zeta_i - \ell^2)^2 + \epsilon^2} \zeta_i^\top Y_i \theta - u_i^\top Z_i \xi + u_i^\top v_i \\ &= -\frac{2\kappa(\zeta_i^\top \zeta_i - \ell^2)}{(\zeta_i^\top \zeta_i - \ell^2)^2 + \epsilon^2} \zeta_i^\top (f_i + g_i u_i - \dot{q}_i) + u_i^\top v_i \\ &\quad - \frac{2\kappa(\zeta_i^\top \zeta_i - \ell^2)}{(\zeta_i^\top \zeta_i - \ell^2)^2 + \epsilon^2} \zeta_i^\top Y_i (\varepsilon_\theta + \hat{\theta}) \\ &\quad - u_i^\top Z_i (\varepsilon_\xi + \hat{\xi}). \end{aligned} \quad (61)$$

Using Assumption 1, there always exists positive constant $\rho_v \in \mathbb{R}_{\geq 0}$ such that for all $t \geq 0$, $\|\dot{q}_i(t)\| \leq \rho_v$. Therefore, we can yield the following inequality from (61)

$$\begin{aligned} \dot{h}_{u,i} &\geq -\frac{2\kappa(\zeta_i^\top \zeta_i - \ell^2)}{(\zeta_i^\top \zeta_i - \ell^2)^2 + \epsilon^2} \zeta_i^\top (f_i + g_i u_i - \dot{q}_i) + u_i^\top v_i \\ &\quad - \frac{2\kappa(\zeta_i^\top \zeta_i - \ell^2)}{(\zeta_i^\top \zeta_i - \ell^2)^2 + \epsilon^2} \zeta_i^\top Y_i \hat{\theta} - u_i^\top Z_i \hat{\xi} \\ &\quad - \left\| \frac{2\kappa(\zeta_i^\top \zeta_i - \ell^2)}{(\zeta_i^\top \zeta_i - \ell^2)^2 + \epsilon^2} \zeta_i^\top Y_i \right\| \|\varepsilon_\theta\| - \|u_i^\top Z_i\| \|\varepsilon_\xi\| \\ &\quad - \left\| \frac{2\kappa(\zeta_i^\top \zeta_i - \ell^2)}{(\zeta_i^\top \zeta_i - \ell^2)^2 + \epsilon^2} \zeta_i \right\| \rho_v. \end{aligned} \quad (62)$$

Define $\tilde{h}_{u,i} = \dot{h}_{u,i} + \alpha(h_{u,i})$, using (22) and (62), one yields

$$\begin{aligned} \tilde{h}_{u,i} &\geq -\frac{2\kappa(\zeta_i^\top \zeta_i - \ell^2)}{(\zeta_i^\top \zeta_i - \ell^2)^2 + \epsilon^2} \zeta_i^\top (f_i + g_i u_i + Y_i \hat{\theta}) \\ &\quad - \left\| \frac{2\kappa(\zeta_i^\top \zeta_i - \ell^2)}{(\zeta_i^\top \zeta_i - \ell^2)^2 + \epsilon^2} \zeta_i \right\| (\|Y_i\| \nu + \rho_v) \\ &\quad - u_i^\top Z_i \hat{\xi} - \|u_i^\top Z_i\| \eta + u_i^\top v_i + \alpha(h_{u,i}). \end{aligned} \quad (63)$$

□

The proof of Lemma 3 is provided as follows.

Proof. We begin with defining a sufficiently smooth function $\tilde{h}_{c,i,k}$:

$$\tilde{h}_{c,i,k} = \ddot{h}_{c,i,k} + \iota_i \dot{h}_{c,i,k} + \alpha(h_{c,i,k}) \quad (64)$$

as a HOCBF with relative degree $r = 2$ of the CBFs $h_{c,i,k}$ in (17). Then, to prove Lemma 3, one needs to show that $\dot{h}_{c,i,k}(t) \geq 0$ for all $t > 0$ and all $k \in \mathcal{I}_k$, such that $h_{c,i,k}(t) \geq 0$ for all $t \geq 0$. This property holds if $\dot{h}_{c,i,k}$ can be expressed in the form of (or larger than) $-\mu \dot{h}_{c,i,k}$ where $\mu > 0$ with $\dot{h}_{c,i,k}(0) \geq 0$.

By reduction and simplification, we yield

$$\begin{aligned} \dot{h}_{c,i,k} &= 2\zeta_i^\top (f_i + g_i u_i + Y_i(\hat{\theta} + \varepsilon_\theta) - \dot{p}_k), \\ &\geq 2\zeta_i^\top (f_i + g_i u_i) + 2\zeta_i^\top Y_i \hat{\theta} - 2 \|\zeta_i^\top Y_i\| \|\varepsilon_\theta\|, \end{aligned} \quad (65)$$

$$\begin{aligned} \ddot{h}_{c,i,k} &\geq 2\zeta_i^\top (\dot{f}_i + \dot{g}_i u_i) + 2\zeta_i^\top \dot{Y}_i \hat{\theta} - 2 \|\zeta_i^\top \dot{Y}_i\| \|\varepsilon_\theta\| \\ &\quad - 2 \|\zeta_i\| \rho_a + 2\zeta_i^\top g_i Z_i \hat{\xi} - \|\zeta_i^\top g_i Z_i\| \|\varepsilon_\xi\| - 2\zeta_i^\top g_i v_i \end{aligned} \quad (66)$$

By using (22) and applied Lemma 1 to (65) and (66), we yield

$$\dot{h}_{c,i,k} \geq 2\zeta_i^\top (f_i + g_i u_i) + 2\zeta_i^\top Y_i \hat{\theta} - 2 \|\zeta_i^\top Y_i\| \nu, \quad (67)$$

$$\begin{aligned} \ddot{h}_{c,i,k} &\geq 2\zeta_i^\top (\dot{f}_i + \dot{g}_i u_i) + 2\zeta_i^\top \dot{Y}_i \hat{\theta} - \|\zeta_i^\top \dot{Y}_i\| \nu \\ &\quad - 2 \|\zeta_i\| \rho_a + 2\zeta_i^\top g_i Z_i \hat{\xi} - \|\zeta_i^\top g_i Z_i\| \eta \\ &\quad - 2\zeta_i^\top g_i v_i \end{aligned} \quad (68)$$

Using (67) and (68), we yield

$$\begin{aligned} \dot{h}_{c,i,k} &\geq 2\zeta_i^\top (\dot{f}_i + \dot{g}_i u_i) + 2\zeta_i^\top \dot{Y}_i \hat{\theta} - \|\zeta_i^\top \dot{Y}_i\| \nu \\ &\quad - 2 \|\zeta_i\| \rho_a + 2\zeta_i^\top g_i Z_i \hat{\xi} - \|\zeta_i^\top g_i Z_i\| \eta \\ &\quad - 2\zeta_i^\top g_i v_i \\ &\quad + \nu_k \left(2\zeta_i^\top (f_i + g_i u_i) + 2\zeta_i^\top Y_i \hat{\theta} \right. \\ &\quad \left. - 2 \|\zeta_i^\top Y_i\| \nu \right) + \alpha(h_{c,i,k}(x_i)) \end{aligned} \quad (69)$$

□

REFERENCES

- [1] Eun S Lee, Donguk Kim, and Seog Y Jeong. Triangular dq tx coils of wireless ev chargers for large misalignment tolerances. *IEEE Transactions on Vehicular Technology*, 72(11):14179–14188, 2023.
- [2] Euihoon Chung and Jung-Ik Ha. Impedance matching network design for 6.78 mhz wireless power transfer system with constant power characteristics against misalignment. *IEEE Transactions on Power Electronics*, 2023.
- [3] Vishnu S Chipade and Dimitra Panagou. Aerial swarm defense using interception and herding strategies. *IEEE Transactions on Robotics*, 2023.
- [4] Vishnu S Chipade and Dimitra Panagou. Multiagent planning and control for swarm herding in 2-d obstacle environments under bounded inputs. *IEEE Transactions on Robotics*, 37(6):1956–1972, 2021.
- [5] Ruilong Zhang, Qun Zong, Xiuyun Zhang, Liqian Dou, and Bailing Tian. Game of drones: Multi-uav pursuit-evasion game with online motion planning by deep reinforcement learning. *IEEE Transactions on Neural Networks and Learning Systems*, 34(10):7900–7909, 2022.
- [6] Jianan Li, Zian Ning, Shaoming He, Chang-Hun Lee, and Shiyu Zhao. Three-dimensional bearing-only target following via observability-enhanced helical guidance. *IEEE Transactions on Robotics*, 39(2):1509–1526, 2022.
- [7] Tiago Oliveira, A. Pedro Aguiar, and Pedro Encarnação. Moving path following for unmanned aerial vehicles with applications to single and multiple target tracking problems. *IEEE Transactions on Robotics*, 32, 08 2016.
- [8] Logan Numerow, Andrea Zanelli, Andrea Carron, and Melanie N Zeilinger. Inherently robust suboptimal mpc for autonomous racing with anytime feasible sqp. *IEEE Robotics and Automation Letters*, 2024.
- [9] Xiaoxiao Li, Zhihao Xu, Shuai Li, Zerong Su, and Xuefeng Zhou. Simultaneous obstacle avoidance and target tracking of multiple wheeled mobile robots with certified safety. *IEEE transactions on cybernetics*, 52(11):11859–11873, 2021.
- [10] Qian Zou, Xingzhou Du, Yuezhen Liu, Hui Chen, Yibin Wang, and Jiangfan Yu. Dynamic path planning and motion control of microbotic swarms for mobile target tracking. *IEEE Transactions on Automation Science and Engineering*, 20(4):2454–2468, 2022.
- [11] Kim Peter Wabersich and Melanie N Zeilinger. A predictive safety filter for learning-based control of constrained nonlinear dynamical systems. *Automatica*, 129:109597, 2021.
- [12] Yifan Hu, Junjie Fu, and Guanghui Wen. Safe reinforcement learning for model-reference trajectory tracking of uncertain autonomous vehicles with model-based acceleration. *IEEE Transactions on Intelligent Vehicles*, 8(3):2332–2344, 2023.
- [13] Danilo Saccani, Leonardo Cecchin, and Lorenzo Fagiano. Multitrajectory model predictive control for safe uav navigation in an unknown environment. *IEEE Transactions on Control Systems Technology*, 31(5):1982–1997, 2022.
- [14] Shaoru Chen, Kong Yao Chee, Nikolai Matni, M Ani Hsieh, and George J Pappas. Safety filter design for neural network systems via convex optimization. In *2023 62nd IEEE Conference on Decision and Control (CDC)*, pages 6356–6363. IEEE, 2023.
- [15] Kai-Chieh Hsu, Haimin Hu, and Jaime F Fisac. The safety filter: A unified view of safety-critical control in autonomous systems. *Annual Review of Control, Robotics, and Autonomous Systems*, 7, 2023.
- [16] Shiyu Chen, Yanjie Li, Yunjiang Lou, Ke Lin, and Xinyu Wu. Learning agile quadrotor flight in restricted environments with safety guarantees. *IEEE Transactions on Intelligent Vehicles*, 2024.
- [17] Mukhtar Sani, Bogdan Robu, and Ahmad Hably. Limited information model predictive control for pursuit-evasion games. In *2021 60th IEEE Conference on Decision and Control (CDC)*, pages 265–270. IEEE, 2021.
- [18] Nianyi Sun, Jin Zhao, Qing Shi, Chang Liu, and Peng Liu. Moving target tracking by unmanned aerial vehicle: A survey and taxonomy. *IEEE Transactions on Industrial Informatics*, 2024.
- [19] Aaron D Ames, Samuel Coogan, Magnus Egerstedt, Gennaro Notomista, Koushil Sreenath, and Paulo Tabuada. Control barrier functions: Theory and applications. In *2019 18th European control conference (ECC)*, pages 3420–3431. IEEE, 2019.
- [20] Aaron D Ames, Gennaro Notomista, Yorai Wardi, and Magnus Egerstedt. Integral control barrier functions for dynamically defined control laws. *IEEE control systems letters*, 5(3):887–892, 2020.
- [21] Gennaro Notomista and Matteo Saveriano. Safety of dynamical systems with multiple non-convex unsafe sets using control barrier functions. *IEEE Control Systems Letters*, 6:1136–1141, 2021.
- [22] Yuxiang Zhang, Xiaoling Liang, Dongyu Li, Shuzhi Sam Ge, Bingzhao Gao, Hong Chen, and Tong Heng Lee. Adaptive safe reinforcement learning with full-state constraints and constrained adaptation for autonomous vehicles. *IEEE Transactions on Cybernetics*, 54(3):1907–1920, 2023.
- [23] Chao Jiang and Yi Guo. Incorporating control barrier functions in distributed model predictive control for multi-robot coordinated control. *IEEE Transactions on Control of Network Systems*, 2023.
- [24] Xiucan Huang, Changyun Wen, and Yongduan Song. Adaptive neural control for uncertain constrained pure feedback systems with severe sensor faults: A complexity reduced approach. *Automatica*, 147:110701, 2023.
- [25] Hsin-Ai Hung, Hao-Huan Hsu, and Teng-Hu Cheng. Image-based multi-uav tracking system in a cluttered environment. *IEEE Transactions on Control of Network Systems*, 9(4):1863–1874, 2022.
- [26] Max H Cohen and Calin Belta. High order robust adaptive control barrier functions and exponentially stabilizing adaptive control lyapunov functions. In *2022 American Control Conference (ACC)*, pages 2233–2238. IEEE, 2022.
- [27] Anup Parikh, Rushikesh Kamalapurkar, and Warren E Dixon. Integral concurrent learning: Adaptive control with parameter convergence using finite excitation. *International Journal of Adaptive Control and Signal Processing*, 33(12):1775–1787, 2019.
- [28] William W Hager. Lipschitz continuity for constrained processes. *SIAM Journal on Control and Optimization*, 17(3):321–338, 1979.
- [29] Jarne JH van Gemert, Mircea Lazar, and Siep Weiland. On unifying control barrier and lyapunov functions using qp and sontag’s formula with an application to tumor dynamics. *arXiv preprint arXiv:2403.14226*, 2024.
- [30] Tuomas Haarnoja, Aurick Zhou, Pieter Abbeel, and Sergey Levine. Soft actor-critic: Off-policy maximum entropy deep reinforcement. In *Proceedings of the 35th International Conference on Machine Learning. July 10th-15th, Stockholm, Sweden*, volume 1870, 1861.
- [31] Michael O’Connell, Guanya Shi, Xichen Shi, Kamyar Azizzadenesheli, Anima Anandkumar, Yisong Yue, and Soon-Jo Chung. Neural-fly enables rapid learning for agile flight in strong winds. *Science Robotics*, 7(66):eabm6597, 2022.